Normal-repeat-length polyglutamine peptides accelerate aggregation nucleation and cytotoxicity of expanded polyglutamine proteins

Natalia Slepko, Anusri M. Bhattacharyya, George R. Jackson, Joan S. Steffan, J. Lawrence Marsh, Leslie Michels Thompson, and Ronald Wetzel

PNAS 2006;103;14367-14372; originally published online Sep 15, 2006;
doi:10.1073/pnas.0602348103

Normal-repeat-length polyglutamine peptides accelerate aggregation nucleation and cytotoxicity of expanded polyglutamine proteins

Natalia Slepko[†], Anusri M. Bhattacharyya[‡], George R. Jackson[§], Joan S. Steffan[†], J. Lawrence Marsh[¶], Leslie Michels Thompson[†‖], and Ronald Wetzel[‡††]

Departments of [†]Psychiatry and Human Behavior and [‖]Biological Chemistry, University of California, Irvine, CA 92697-4260; [‡]Graduate School of Medicine, University of Tennessee, Knoxville, TN 37920; [§]Department of Neurology, David Geffen School of Medicine, University of California, Los Angeles, CA 90095; and [¶]Developmental Biology Center and Department of Developmental and Cell Biology, University of California, Irvine, CA 92697-2300

Edited by Sue Hengren Wickner, National Institutes of Health, Bethesda, MD, and approved August 1, 2006 (received for review March 22, 2006)

The dependence of disease risk and age-of-onset on expanded CAG repeat length in diseases like Huntington's disease (HD) is well established and correlates with the repeat-length-dependent nucleation kinetics of polyglutamine (polyGln) aggregation. The wide variation in ages of onset among patients with the same repeat length, however, suggests a role for modifying factors. Here we describe the ability of normal-length polyGln repeat sequences to greatly accelerate the nucleation kinetics of an expanded polyGln peptide. We find that normal-length polyGln peptides enhance the *in vitro* nucleation kinetics of a Q_{47} peptide in a concentration-dependent and repeat-length-dependent manner. *In vivo*, we show that coexpression of a Q_{20} sequence in a *Drosophila* model of HD expressing Htt exon 1 protein with an Q_{93} repeat accelerates both aggregate formation and neurotoxicity. The accelerating effect of short polyGln peptides is attributable to the promiscuity of polyGln aggregate elongation and reflects the intimate relationship between nucleus formation and early elongation events in establishing nucleation kinetics. The results suggest that the overall state of the polyGln protein network in a cellular environment may have a profound effect on the toxic consequences of polyGln expansion and thus may serve as a genetic modifier of age of onset in HD.

Drosophila | Huntington's disease | *in vitro* | elongation kinetics | amyloid

A hallmark feature of neurodegenerative disorders such as Huntington's disease and other expanded polyglutamine (polyGln) repeat diseases (1) is the appearance, in subsets of neurons, of visible aggregates made up of the mutant disease protein and other cellular proteins, including other polyGln repeat proteins. A role for aggregation in disease also is suggested by the close agreement between the repeat-length dependence of aggregation (2, 3) and the repeat-length dependence of disease risk for most polyGln repeat diseases (1). Tracing the role of aggregates in disease is complicated, however, by the variety of aggregate sizes, morphologies, and functionalities observed in cells and tissue (4). For example, depending on conditions, polyGln-containing molecules can make either mature amyloid fibrils (5–7) or oligomeric structures (8–10). This variety of aggregate types may help explain the lack of an apparent relationship between visible aggregates and physiological consequences in some cell and animal studies (11).

Most protein aggregation reactions occur through either colloidal coagulation (12, 13) or nucleated growth (14) pathways. Spontaneous aggregation of simple polyGln peptides occurs via a classic nucleation-dependent polymerization pathway (15). The nucleus for polyGln amyloid formation appears to be an alternatively folded state of the monomer (15) that exists in a highly unfavorable preequilibrium with the bulk-phase, disordered monomer (16). Once polyGln amyloid fibrils have formed, they grow by means of a highly efficient elongation reaction (15, 16). Although elongation of amyloid fibrils is generally highly selective, so that incorporation of other sequences into growing aggregates is very inefficient (17), polyGln amyloid growth is robustly promiscuous. Thus, qualitative studies with polyGln-containing proteins (18, 19) and quantitative studies with simple polyGln sequences (3) indicate that any protein with a sterically accessible polyGln segment can serve to elongate a polyGln-based aggregate. This finding is important in expanded CAG repeat diseases, because, in addition to the nine known polyGln disease proteins (20), the human genome contains a substantial number of other proteins featuring polyGln repeats and Gln-rich sequences (21–23).

We report here the finding that normal-length polyGln sequences can greatly enhance the nucleation phase of the polyGln aggregation reaction. We show that the overall efficiency of nucleation is controlled not only by the thermodynamics of nucleus formation but also by kinetics by which transient nuclei become committed to the aggregation process. Commitment of nuclei to aggregate formation is favored by normal-length polyGln peptides by virtue of the promiscuity of polyGln elongation. We extend these observations to *in vivo* experiments in which coexpression of a short polyGln peptide in a *Drosophila* model of Huntington's disease leads to an acceleration of Htt aggregation that correlates with an acceleration of polyGln toxicity. The results suggest that normal-length, endogenous polyGln proteins in the cellular milieu can significantly influence amyloid formation by an expanded repeat-length polyGln protein, potentially influencing the age of onset for disease. The results also support the thermodynamic model of nucleation in which aggregation nuclei are treated as being formed in a rapid and reversible preequilibrium with bulk-phase monomer (14, 15).

Results

A general depiction of the thermodynamic model for nucleated growth polymerization (14) is shown in Fig. 1. Formation of the nucleus N^* from bulk-phase monomer M_a is modeled as a rapid and reversible, but highly unfavorable, process (15, 16). Once formed, the metastable N^* can either disintegrate back to the monomer pool or elongate, via reaction with additional M_b molecules, to generate lower free-energy reaction mixtures containing N^*_{+1}, N^*_{+2}, etc. The more efficient these elongation

Author contributions: N.S. and A.M.B. contributed equally to this work; N.S., A.M.B., G.R.J., J.S.S., J.L.M., L.M.T., and R.W. designed research; N.S. and A.M.B. performed research; G.R.J. contributed new reagents/analytic tools; N.S., A.M.B., G.R.J., J.S.S., J.L.M., L.M.T., and R.W. analyzed data; and N.S., A.M.B., G.R.J., J.S.S., J.L.M., L.M.T., and R.W. wrote the paper.

The authors declare no conflict of interest.

This paper was submitted directly (Track II) to the PNAS office.

[††]To whom correspondence should be sent at the present address: Department of Structural Biology, University of Pittsburgh School of Medicine, 2044 Biomedical Science Tower 3, 3501 Fifth Avenue, Pittsburgh, PA 15260. E-mail: rwetzel@pitt.edu.

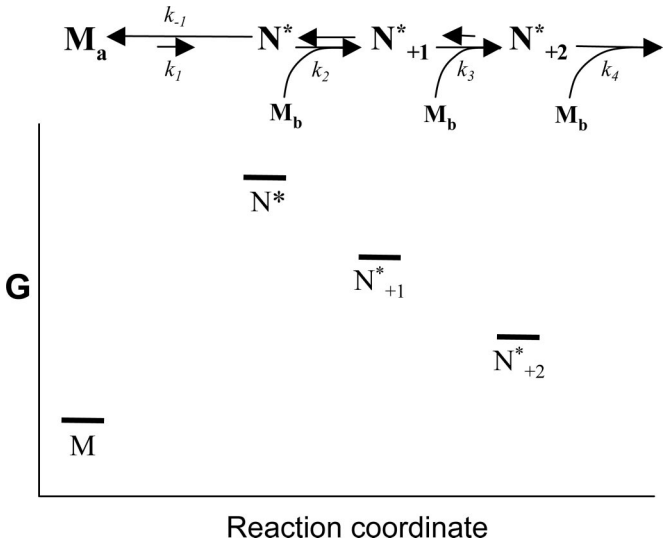

Fig. 1. Nucleation-dependent polymerization mechanism of polyGln aggregation. Formation of nucleus N^* from bulk-phase monomer M_a is modeled as a reversible, highly unfavorable reaction. Once formed, the metastable N^* can either disintegrate back to the monomer pool or elongate by adding M_b molecules to form N^*_{+1}, N^*_{+2}, etc., and by doing so stabilize the system. The term M_b signifies the monomer pool capable of supporting elongation. In most amyloid systems, M_b is identical to M_a, but, as shown in this paper, M_b can be an expanded pool that includes other polyGln sequences. Previously, we showed that the number of molecules of polyGln comprising N^* (called critical nucleus, or n^*) is equal to 1 for nucleation of polyGln aggregation (15); the general aspects of theory and interpretation discussed in this work, however, are independent of the molecularity of N^*.

steps, the more likely a transiently formed nucleus will be channeled essentially irreversibly into aggregate formation. In principle, any M_b capable of elongation of N^* promotes nucleation, by increasing the effectiveness with which elongation competes with disintegration of N^*. This trend is implicit in the simplified equation describing nucleation, $\Delta = 1/2k_+^2 K_{n^*} c^{(n^*+2)} t^2$, in which the concentration of monomers converted to aggregates at time t depends on the square of the elongation rate constant k_+ (14, 15). Thus, although the nucleation phase of nucleated growth is normally considered as being separate from the elongation phase, the thermodynamic model of nucleation suggests that the kinetics of the elongation reactions operating on the nucleus and early aggregates will contribute to the overall kinetics of nucleation.

Because the polyGln amyloid system exhibits promiscuity of aggregate elongation by different polyGln peptides, the thermodynamic model of nucleation predicts that relatively short polyGln molecules, even those too short to effectively undergo nucleation themselves, should be effective promoters of the nucleation of expanded polyGln sequences. Thus, normal-length polyGln peptides in the environment are predicted to increase the percentage of times that newly formed nuclei progress toward aggregation rather than decay back to bulk-phase monomer. Furthermore, the efficiency with which other polyGln sequences augment nucleation is predicted to depend on both the repeat lengths and concentrations of these additional polyGln sequences.

Normal-Length polyGln Peptides Enhance Aggregation Nucleation of an Expanded polyGln Peptide *in Vitro*. To test the above hypothesis, we followed the early aggregation kinetics of the simple polyGln peptide Q_{47} in the presence of different concentrations of the normal-repeat-length peptide Q_{20}. At 1.8 μM and 37°C in PBS, this Q_{47} peptide alone does not aggregate for up to 6 days (Fig. 2*a*; only data up to 6 h are shown). However, in the presence of low micromolar concentrations of the Q_{20} peptide, aggregation of a 1.8 μM solution of Q_{47} is observable within a few hours, and

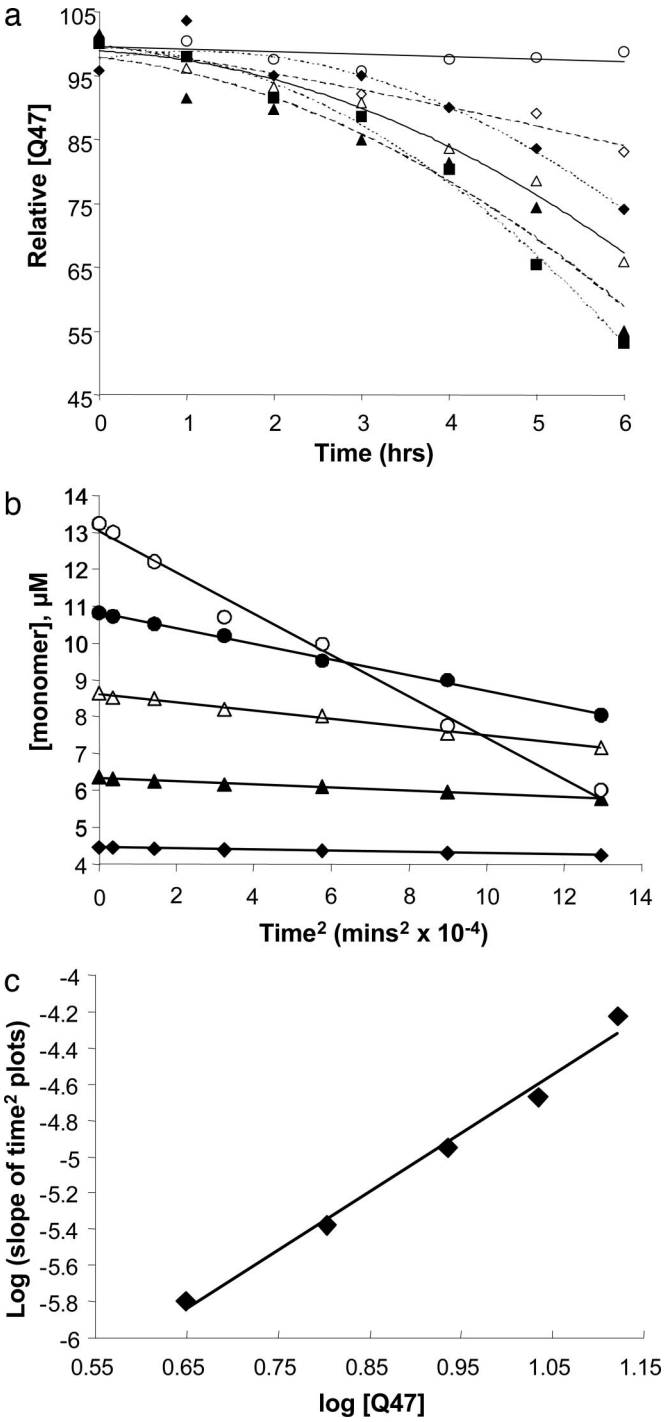

Fig. 2. The effect of a short polyGln peptide on the nucleation of a polyGln of pathological length. (*a*) PolyGln Q_{47} was incubated at 37°C at 1.8 μM, either alone (○) or in the presence of various concentrations of Q_{20}: 14 μM (◇), 24 μM (◆), 36 μM (△), 44 μM (▲), and 54 μM (■). The disappearance of Q_{47} from the soluble phase is shown on a relative basis for each reaction mixture. (*b*) t^2 plots (14) of the nucleation kinetics of various concentrations of Q_{47} in the presence of 18 μM Q_{20}. Starting concentrations of Q_{47} were 13.2 (○), 10.8 (●), 8.6 (△), 6.4 (▲), and 4.5 (◆) μM. (*c*) Concentration dependence of nucleation kinetics, plotting the logarithm of the slopes of the t^2 plots from *b* versus log[Q_{47}]. The slope m of the linear regression fit is 3.2, $R^2 = 0.9881$; N^* is calculated to be 1.2 ($N^* = m - 2$) (15).

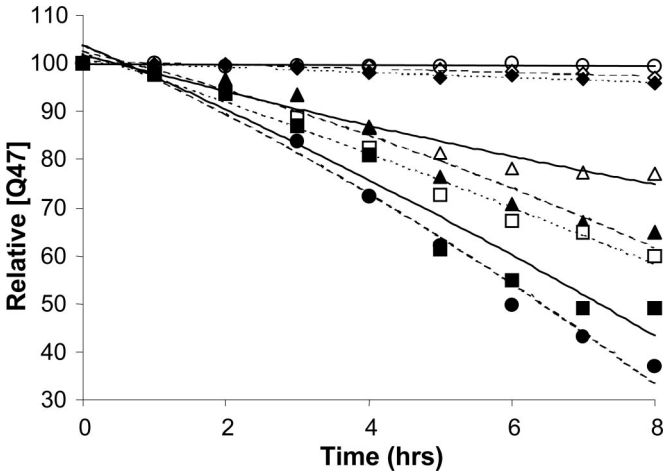

Fig. 3. The role of repeat length on the augmentation of Q_{47} aggregation nucleation by shorter polyGln sequences. Samples of 1.5–2.0 μM Q_{47} were incubated either alone (○) or with 20 μM polyGln peptides of various repeat lengths: Q_{10} (◇), Q_{15} (◆), Q_{20} (△), Q_{25} (▲), Q_{29} (□), Q_{33} (■), or Q_{40} (●). The disappearance of Q_{47} from the soluble phase is shown on a relative basis for each reaction mixture.

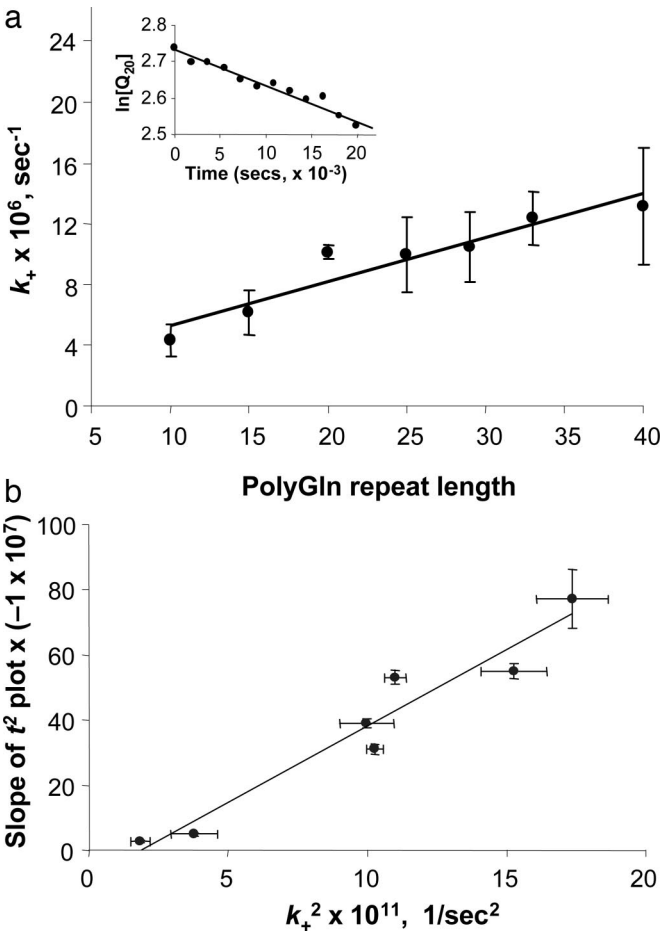

Fig. 4. The role of elongation kinetics in aggregation nucleation. (*a*) Rates of elongation of 2.3 μg/ml Q_{47} amyloid fibrils by 17 μM monomeric polyGln plotted against the repeat length of the monomeric polyGln. (*Inset*) Pseudofirst-order rate plot for the elongation of 17 μM Q_{20}; because the molar concentration of fibrils does not change in a simple fibril elongation reaction, elongation kinetics are pseudofirst-order (39), yielding a pseudofirst-order rate constant that is an amalgam of the true second-order rate constant and the molar concentration of fibrils. (*b*) A plot of the slope of the t^2 plot for Q_{47} nucleation (Fig. 3) with respect to the square of the rate constants k_+, describing the elongation of each short polyGln peptide (from *a*). [We used the square of the rate constant here because of the dependence of nucleation kinetics on the second power of the elongation rate, as shown in the equation $\Delta = 1/2k_+^2K_{n^*}c^{(n^*+2)}t^2$ (14, 15).]

higher concentrations of Q_{20} further increase Q_{47} aggregation (Fig. 2*a*). In comparison, incubation of neither Q_{20} alone at 100 μM or Q_{47} alone at 7 μM produces any aggregation at 6 hours; to obtain the degree of aggregation of Q_{47} observed after 6 h with 1.8 μM Q_{47}/36 μM Q_{20} (Fig. 2*a*, ◇), it is necessary to incubate 15 μM Q_{47} (data not shown).

Analysis (14, 15) of the aggregation kinetics shows that Q_{47} in the presence of different amplifying concentrations of Q_{20} exhibits the defining features of a nucleated growth polymerization pathway: (*i*) disappearance of monomeric Q_{47} from solution in the early phases of aggregation follows t^2 kinetics (Fig. 2*b*) and (*ii*) the logarithms of the slope of the t^2 plots trending linearly with the logarithms of starting Q_{47} concentrations (Fig. 2*c*). As previously found for aggregation of homogeneous repeat-length polyGln solutions (15), the slope of the logarithm–logarithm plot corresponds to a critical nucleus of 1 (see legend to Fig. 2). Thus, the presence of Q_{20} does not cause a change in mechanism but rather changes the overall nucleation kinetics.

Previously we showed that polyGln repeat length influences the rates of elongation reactions (3). If normal-length polyGln peptides accelerate Q_{47} nucleation by increasing the rate of nucleus elongation, we would therefore expect that, for any polyGln concentration, acceleration should increase as the repeat length of the added peptide increases. We incubated Q_{47} (1.5–2.0 μM) plus short polyGln of various repeat lengths (≈17 μM). As expected, the nucleation kinetics of Q_{47} aggregation are enhanced as the repeat length of the added polyGln increases (Fig. 3). Short (10–15 aa) repeat length polyGln peptides give modest but measurable acceleration. Thereafter, acceleration increases as repeat length increases. The mechanism of the length-dependent effect also appears to be an enhancement of the normal nucleation mechanism, because linear t^2 plots were obtained for Q_{47} incorporation into aggregates in the presence of all of these short polyGln peptides (data not shown).

To further probe whether our results are consistent with the thermodynamic nucleation model (Fig. 1), we determined the pseudofirst order (see legend to Fig. 4) rate constants for the elongation of preformed Q_{47} aggregate seeds by polyGln peptides of different repeat lengths (see, for example, Fig. 4*a Inset*). In accord with previous results (3), we found that the elongation rate constants for these reactions increase as repeat length increases (Fig. 4*a*). We then plotted the nucleation rate parameter (the t^2 slopes from Fig. 3) for each accelerating peptide against the square of the corresponding repeat-length-dependent elongation rate constant (from Fig. 4*a*). The resulting plot (Fig. 4*b*) shows a linear dependence throughout the repeat-length range, consistent with the hypothesis that the accelerating effect of short polyGln sequences on nucleation kinetics of expanded polyGln peptides simply is due to the influence that repeat length exerts over the elongation rate. This finding supports the thermodynamic model (Fig. 1).

Expression of a Short polyGln Peptide Accelerates Aggregation in a *Drosophila* Model of polyGln Toxicity. These *in vitro* kinetics results suggest that a given concentration of an expanded polyGln repeat protein would be more likely to form aggregates in a cell that is rich in normal-repeat-length polyGln sequences. To test this hypothesis, we coexpressed a Q_{20} version of Htt exon 1 (Httex1p-Q_{20}) together with a Q_{93} form (Httex1p-Q_{93}) (24, 25)

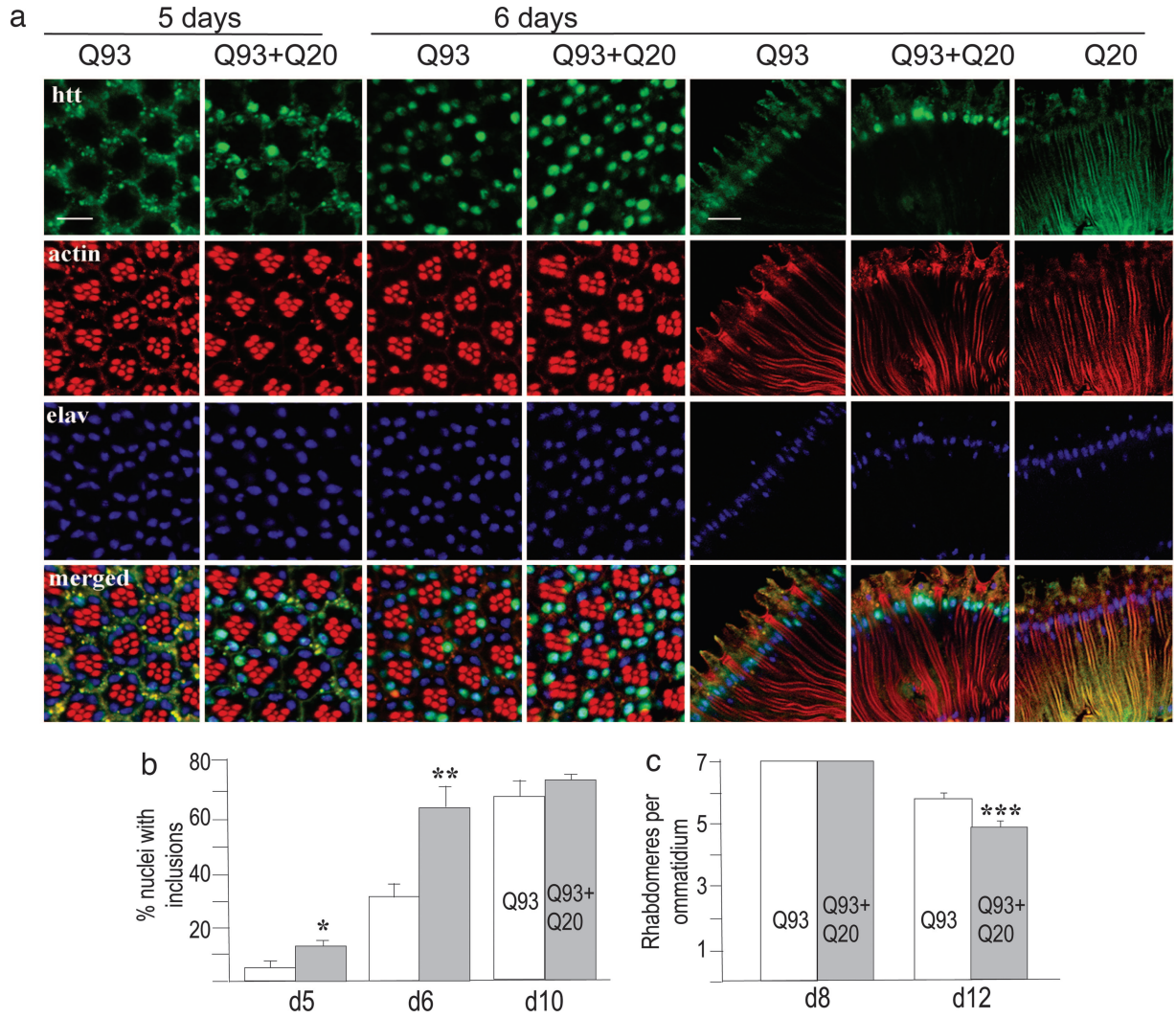

Fig. 5. Coexpression of Httex1p-Q_{20}p increases formation of nuclear inclusions and toxicity of Httex1p-Q_{93}p. (*a*) Confocal images of *Drosophila* eye expressing polyGln transgenes in adult photoreceptor neurons. Htt accumulation is green, rhabdomeres of photoreceptor neurons are red by anti-actin staining, and photoreceptor nuclei are blue by staining with anti-elav antibody. The first four columns of photographs show cross-sections at days 5 and 6. (Scale bar: 10 μM.) The last three columns of photographs show longitudinal sections through the eye at day 6. (Scale bar: 20 μM.) Extensive staining of cytoplasmic Htt is seen at day 5 and is primarily converted to nuclear staining in 6-day-old flies. At each time point, where Q_{20} is coexpressed with Q_{93}, an increase in the number of visible inclusions is observed. No aggregates are observed with Q_{20} alone. (*b*) The number of photoreceptor nuclei with visible inclusions in 5-, 6-, and 10-day-old flies (d5, d6, and d10, respectively). The fraction of nuclei with inclusions at days 5 and 6 is increased when Q_{20} is coexpressed; however, the percentage of nuclei with inclusions with and without Q_{20} coexpression plateaus by day 10. The percentage of nuclear accumulation was calculated as Htt-positive nuclei per all nuclei per field [*, $P < 0.025$ (0.0239); **, $P < 0.015$ (0.0145)]. (*c*) Pathology is evaluated by comparing the number of rhabdomeres per ommatidium in 8-day-old (d8) and 12-day-old (d12) flies [***, $P < 0.0015$ (0.00141)]. No neurotoxicity is observed up to day 8, but toxicity is evident by day 12 and is increased by the presence of Q_{20}.

in *Drosophila*. A rhodopsin driver (Rh→GAL4) that drives transgene expression in six (R1–R6) of eight photoreceptor neurons of each ommatidium in adult flies was used. Five days after onset of transgene expression of Httex1p-Q_{93} alone, the protein is found primarily in the cytosol in multiple, small aggregates (Fig. 5*a*). Twenty-four hours later, at day 6, nuclear aggregates began to appear. By day 10, most nuclei contained nuclear inclusions (Fig. 5*b*). In contrast, no visible aggregates were observed at any time in flies expressing Httex1p-Q_{20} alone (Fig. 5*a* and data not shown). However, when the Q_{20} protein was coexpressed with the Q_{93} form, more cells with nuclear inclusions were evident when analyzed at days 5 and 6 [compare 5% of cell nuclei with inclusions in flies expressing Q_{93} alone to 13% in flies expressing Q_{93} plus Q_{20} at day 5, and, likewise, 32% to 65% at day 6 (Fig. 5*b*)]. By day 10, almost all cell nuclei in flies expressing both Q_{93} and Q_{93} plus Q_{20} contained inclusions, and the difference between the two lines was no longer observed (Fig. 5*b*). These results are consistent with an increased rate of spontaneous polyGln aggregation due to enhanced nucleation.

Expression of a Short polyGln Peptide Accelerates Neurodegeneration in a *Drosophila* Model of polyGln Toxicity. To determine whether the increased rate of aggregation correlates with an increase in pathology, we compared the number of surviving photoreceptor neurons in flies expressing Httex1p-Q_{93} vs. Httex1p-Q_{20} plus Httex1p-Q_{93}. By as late as 8 days after eclosion, flies expressing Httex1p-Q_{93} alone had seven intact rhabdomeres (the light gathering organ of the photoreceptors) visible by pseudopupil analysis (26), similar to wild-type flies (Fig. 5*a* and data not shown). By day 12, the average number of rhabdomeres per ommatidium decreased to 5.8 (Fig. 5*c*), indicating mild degeneration. When Httex1p-Q_{93} was coexpressed with Httex1p-Q_{20},

neuronal degeneration at 12 days was increased, with an average of only 4.7 rhabdomeres per ommatidium remaining (Fig. 5*c*). Thus, the accelerated rate of aggregate formation observed in response to coexpression with Httex1p-Q_{20} correlates with an increase in neuronal degeneration.

Discussion

The results presented here show that short polyGln peptides, without changing the nucleation mechanism, exert a strong accelerating effect on the nucleation kinetics of an expanded polyGln, an effect that depends on repeat length and concentration. This rate enhancement is reflected in an accelerated appearance of visible aggregates *in vivo* in a *Drosophila* model of Huntington's disease, which in turn is correlated with enhanced degeneration of photoreceptor neurons in adult flies.

The accelerating effect of nonpathogenic polyGln peptides on the nucleation kinetics of an expanded pathogenic polyGln derives from the ability of these short peptides to elongate aggregation nuclei and nascent aggregates. Because the nature of the aggregation nucleus is itself unchanged, acceleration of nucleation by short polyGln sequences might best be considered a kind of assisted homogenous nucleation. Our studies (15, 16, 27) of polyGln aggregation nucleation kinetics are based on a nucleated growth polymerization model in which the nucleus exists in a rapid preequilibrium with the bulk-phase pool of monomers (Fig. 1) and is defined as the least thermodynamically stable species on the aggregation pathway (14). The observations reported here provide strong support for this model. If formation of a nucleus from bulk-phase monomer were kinetically rate-limiting (that is, a very small k_1 in Fig. 1), then enhancing the rates of subsequent elongation steps would not be expected to increase the overall nucleation rate. Because we show here that enhancing the early elongation steps enhances the efficiency of nucleation, we conclude that formation of the nucleus itself is a rapid preequilibrium in which (in the absence of added, short-repeat-length polyGln) $[M_a]k_1 \gg [M_a][N^*]k_2$.

These results are strictly valid only for spontaneous aggregation reactions that proceed through a nucleated growth polymerization pathway. Although this mechanism holds for simple polyGln peptides, the growth of most other amyloid fibrils appears to involve oligomeric and protofibrillar species whose mechanisms of formation, growth, and conversion into mature amyloid are still being worked out. Besides the nine proteins currently implicated in different polyGln expansion diseases (1), the human genome encodes many other proteins containing polyGln sequences of various repeat lengths (21–23). The analysis described here suggests that genetic modifiers of adult age-of-onset, predicted by human studies (28–30), may include variation in either the concentrations and/or repeat lengths of some of these sequences to directly influence the aggressiveness of expanded repeat polyGln aggregation and disease. For example, the accelerating effect of normal-length polyGln sequences on polyGln aggregation nucleation and toxicity may help explain how overexpression of the polyGln-containing CREB-binding protein can in some animal and cellular models exacerbate expanded polyGln toxicity (Pedro Fernandez-Funez and Juan Botas, personal communication; and N.S., J.S.S., G.R.J., J.L.M. and L.M.T., unpublished data) while being protective in other cases (31, 32). Likewise, the aggressiveness of an expanded polyGln disease might be stimulated by increases in concentration or repeat length of other polyGln disease proteins within the subcellular environment, as has recently been suggested by a genetics analysis of spinocerebellar ataxia 2 (33).

If the hypothesis developed in this paper has merit, it will be especially important to understand the steady-state concentrations, state of proteolytic fragmentation, and cellular and subcellular distributions of all members of this polyGln protein network, not just of molecules with repeat lengths near or above the pathological threshold. More broadly, it will be important to understand all of the factors influencing the formation of various polyGln aggregates if we are to fully describe the molecular mechanisms of these diseases and confidently devise treatment strategies.

Experimental Procedures

***In Vitro* Kinetics Analysis.** All peptides were obtained by custom synthesis from the Keck Center at Yale University (New Haven, CT). All synthetic polyGln peptides include pairs of Lys residues at the N and C termini for solubility (7). All procedures have been described in detail previously (34, 35). Peptides were purified by reverse-phase HPLC, pooled with the aid of mass spectrometric characterization of chromatography fractions, lyophilized, and stored at −80°C (34). Before use in an aggregation reaction, peptides were disaggregated by using reversible exposure to organic solvents (34–36). Peptide concentrations were determined by using a centrifugation–HPLC sedimentation assay (34, 35); HPLC separation allows independent analysis of Q_{47} peptides in the presence of shorter peptides. Kinetics experiments were set up by dilution into PBS of freshly disaggregated peptide stocks. Aggregates used as seeds were grown (7), harvested, and characterized as described (35). Nucleation kinetics analysis was as described previously (15, 34, 35).

***Drosophila* Stocks and Crosses.** The polyGln-expressing transgenic stocks used in this study were *w*; P{UAS-Httex1p Q93}4F1 and *w*; P{UAS-Httex1p Q20}111M1 (24, 25). These flies were mated with an *Rh1*-Gal4 driver line (37) in which the rhodopsin promoter drives transgene expression in adult photoreceptors R1–R6 (a kind gift from C. Desplan, New York University, New York, NY). Cultures were raised at 29°C.

Pseudopupil Analysis. Flies 8 and 12 d old were decapitated and mounted in a drop of nail polish on a microscopic slide as described previously (24, 25). The head was then covered with immersion oil and examined under a Nikon (Tokyo, Japan) EFD-3 Optiphot-2 scope with ×50 oil objective. At least 50 ommatidia in 4 flies were examined, and the number of visible rhabdomeres was counted for each.

Immunochemistry and Confocal Analysis. Heads of adult flies were prefixed in 4% formaldehyde at room temperature for 1 h, and eyes were dissected in PBS. The tissue was fixed for an additional 10 min in formaldehyde at room temperature. After permeabilization and blocking (0.2% Triton X-100 in PBS for 2 h at room temperature and 5% normal goat serum/0.2% Triton X-100 in PBS at 2 h at room temperature), tissues were incubated with primary antibody in blocking solution overnight at 4°C. After washing in blocking buffer, secondary antibody was applied for 2 h at room temperature. The primary antibodies were anti-Htt S830 (1:1,000 dilution; gift from G. Bates, King's College London School of Medicine, London, U.K.) (38) and anti-elav (1:200 dilution; Iowa Hybridoma Bank, University of Iowa, Iowa City, IA). Rhabdomeres of adult photoreceptors were visualized by staining F-actin with 2 ng/ml TRITC-phalloidin (Sigma, St. Louis, MO). Secondary antibodies at 1:200 dilutions were from Jackson ImmunoResearch (West Grove, PA). The photographs featured in Fig. 5 are from a single confocal (model no. LSM510; Zeiss, Thornwood, NY) section through the eye. The position of section (cross-sections and longitudinal sections) was chosen at the level of photoreceptor nuclei localization.

Quantitation of Inclusions. Visual counts of nuclear inclusions and neuronal nuclei were performed by using images obtained by confocal microscopy. Every image was taken from one individual

eye, and five to seven animals were analyzed. For each data point, 500–800 cells were counted. Aggregation is expressed as the percentage of nuclei with inclusions versus the total number of nuclei per field.

We thank Frank Ferrone for reviewing the manuscript, Barbara Apostol for assistance with the figures, C. Desplan for the generous gift of Rh1-Gal4 flies, and G. Bates for the anti-Htt S830 antibody. The anti-elav antibody was obtained from the Developmental Studies Hybridoma Bank. We also gratefully acknowledge Optical Biology Shared Resource of Cancer Centre Support Grant CA-62203 from the University of California. This work were supported by U.S. Public Health Service Grants R01 AG19322 (to R.W.) and NS-45283 (to J.L.M.), a Hereditary Disease Foundation postdoctoral fellowship (to N.S.), the Hereditary Disease Foundation (L.M.T.), the Huntington's Disease Society of America (L.M.T. and J.L.M.), and the HighQ Foundation (J.L.M. and L.M.T.).

1. Bates GP, Benn C (2002) in *Huntington's Disease*, eds Bates GP, Harper PS, Jones L (Oxford Univ Press, Oxford, UK), pp 429–472.
2. Scherzinger E, Sittler A, Schweiger K, Heiser V, Lurz R, Hasenbank R, Bates GP, Lehrach H, Wanker EE (1999) *Proc Natl Acad Sci USA* 96:4604–4609.
3. Chen S, Berthelier V, Yang W, Wetzel R (2001) *J Mol Biol* 311:173–182.
4. Wetzel R (2006) in *Genetic Instabilities and Neurological Diseases*, eds Wells R, Ashizawa T (Elsevier, San Diego), pp 517–534.
5. DiFiglia M, Sapp E, Chase KO, Davies SW, Bates GP, Vonsattel JP, Aronin N (1997) *Science* 277:1990–1993.
6. Scherzinger E, Lurz R, Turmaine M, Mangiarini L, Hollenbach B, Hasenbank R, Bates GP, Davies SW, Lehrach H, Wanker EE (1997) *Cell* 90:549–558.
7. Chen S, Berthelier V, Hamilton JB, O'Nuallain B, Wetzel R (2002) *Biochemistry* 41:7391–7399.
8. Poirier MA, Li H, Macosko J, Cai S, Amzel M, Ross CA (2002) *J Biol Chem* 277:41032–41037.
9. Kayed R, Head E, Thompson JL, McIntire TM, Milton SC, Cotman CW, Glabe CG (2003) *Science* 300:486–489.
10. Wacker JL, Zareie MH, Fong H, Sarikaya M, Muchowski PJ (2004) *Nat Struct Mol Biol* 11:1215–1222.
11. Arrasate M, Mitra S, Schweitzer ES, Segal MR, Finkbeiner S (2004) *Nature* 431:805–810.
12. Modler AJ, Gast K, Lutsch G, Damaschun G (2003) *J Mol Biol* 325:135–148.
13. Carrotta R, Manno M, Bulone D, Martorana V, San Biagio PL (2005) *J Biol Chem* 280:30001–30008.
14. Ferrone F (1999) *Methods Enzymol* 309:256–274.
15. Chen S, Ferrone F, Wetzel R (2002) *Proc Natl Acad Sci USA* 99:11884–11889.
16. Bhattacharyya AM, Thakur A, Wetzel R (2005) *Proc Natl Acad Sci USA* 102:15400–15405.
17. O'Nuallain B, Williams AD, Westermark P, Wetzel R (2004) *J Biol Chem* 279:17490–17499.
18. Huang CC, Faber PW, Persichetti F, Mittal V, Vonsattel JP, MacDonald ME, Gusella JF (1998) *Somatic Cell Mol Genet* 24:217–233.
19. Perez MK, Paulson HL, Pendse SJ, Saionz SJ, Bonini NM, Pittman RN (1998) *J Cell Biol* 143:1457–1470.
20. Bates GP, Harper PS, Jones L (2002) *Huntington's Disease* (Oxford Univ Press, Oxford, UK).
21. Margolis RL, Abraham MR, Gatchell SB, Li SH, Kidwai AS, Breschel TS, Stine OC, Callahan C, McInnis MG, Ross CA (1997) *Hum Genet* 100: 114–122.
22. Hancock JM, Worthey EA, Santibanez-Koref MF (2001) *Mol Biol Evol* 18:1014–1023.
23. Collins JR, Stephens RM, Gold B, Long B, Dean M, Burt SK (2003) *Genomics* 82:10–19.
24. Steffan JS, Bodai L, Pallos J, Poelman M, McCampbell A, Apostol BL, Kazantsev A, Schmidt E, Zhu YZ, Greenwald M, *et al*. (2001) *Nature* 413:739–743.
25. Agrawal N, Pallos J, Slepko N, Apostol BL, Bodai L, Chang L, Chang A, Thompson LM, Marsh JL (2005) *Proc Natl Acad Sci USA* 102:3777–3781.
26. Franceschini N (1972) in *Information Processing in the Visual Systems of Arthropods*, ed Wehner R (Springer, New York), pp 75–82.
27. Bhattacharyya AM, Thakur AK, Hermann VM, Thiagarajan G, Williams AD, Chellgren BW, Creamer TP, Wetzel R (2006) *J Mol Biol* 355:524–535.
28. Li JL, Hayden MR, Almqvist EW, Brinkman RR, Durr A, Dode C, Morrison PJ, Suchowersky O, Ross CA, Margolis RL, *et al*. (2003) *Am J Hum Genet* 73:682–687.
29. Djousse L, Knowlton B, Hayden MR, Almqvist EW, Brinkman RR, Ross CA, Margolis RL, Rosenblatt A, Durr A, Dode C, *et al*. (2004) *Neurogenetics* 5:109–114.
30. Wexler NS, Lorimer J, Porter J, Gomez F, Moskowitz C, Shackell E, Marder K, Penchaszadeh G, Roberts SA, Gayán J, *et al*. (2004) *Proc Natl Acad Sci USA* 101:3498–3503.
31. Nucifora FC, Jr, Sasaki M, Peters MF, Huang H, Cooper JK, Yamada M, Takahashi H, Tsuji S, Troncoso J, Dawson VL, *et al*. (2001) *Science* 291:2423–2428.
32. Taylor JP, Taye AA, Campbell C, Kazemi-Esfarjani P, Fischbeck KH, Min KT (2003) *Genes Dev* 17:1463–1468.
33. Pulst SM, Santos N, Wang D, Yang H, Huynh D, Velazquez L, Figueroa KP (2005) *Brain* 128:2297–2303.
34. Wetzel R (2005) in *The Protein Folding Handbook*, eds Buchner J, Kiefhaber T (Wiley, Weinheim, Germany), Part II, pp 1170–1214.
35. O'Nuallain B, Thakur AK, Williams AD, Bhattacharyya AM, Chen S, Thiagarajan G, Wetzel R (2006) *Methods Enzymol* 413:34–74.
36. Chen S, Wetzel R (2001) *Protein Sci* 10:887–891.
37. Chyb S, Hevers W, Forte M, Wolfgang WJ, Selinger Z, Hardie RC (1999) *J Neurosci* 19:8799–8807.
38. Smith DL, Portier R, Woodman B, Hockley E, Mahal A, Klunk WE, Li, X.-J., Wanker EE, Murray KD, Bates GP (2001) *Neurobio Dis* 8:1017–1026.
39. Naiki H, Gejyo F (1999) *Methods Enzymol* 309:305–318.